Self-focusing in CS_2 at 10.6 μm

M. Mohebi, P. F. Aiello, G. Reali,* M. J. Soileau, and E. W. Van Stryland

Center for Applied Quantum Electronics, Department of Physics, North Texas State University, Denton, Texas 76203

Received January 28, 1985; accepted May 8, 1985

We have measured the nonlinear refractive index, n_2, of CS_2 at 10.6 μm by observing the onset of whole-beam self-focusing. We find that n_2 is $(2.2 \pm 0.7) \times 10^{-10}$ esu, which is over an order of magnitude larger than n_2 in the visible.

Nonlinear refraction in CS_2 has been studied extensively by many workers using a variety of different techniques at various laser wavelenths and pulse widths.[1-5] In fact, CS_2 has become a standard to which the nonlinear properties of other materials are often referenced. Reasonable agreement is found among the various measurements of the nonlinear index, n_2, for wavelengths ranging from the visible to the near IR. On the other hand, to our knowledge there have been only two studies of the nonlinear refraction in CS_2 at 10.6 μm,[6,7] and the n_2 values reported differ by 3 orders of magnitude. In view of the importance of CO_2 laser sources and the need for a standard against which nonlinear materials can be characterized in the IR, we have undertaken a study of the nonlinear properties of liquid CS_2 in the 10.6-μm spectral region. In this Letter we report the results of the measurements of the critical power for self-focusing (SF) at 10.6 μm. This was accomplished by measuring the power required for the onset of whole-beam SF using optical-power-limiting[4,5] (OPL) and optoacoustic-detection[8] (OAD) techniques.

Figure 1 is a diagram of the experiment. Our measurements were performed using a single longitudinal, single transverse TEM_{00} mode CO_2 laser operating at the $P(20)$ line. We took great care to obtain a stable TEM_{00} mode in order to avoid small-scale SF, and indeed small-scale SF was not observed during the experiment. The output energy was up to 100 mJ, delivered in 130-nsec FWHM pulses. Typical spatial and temporal profiles are shown in Fig. 1. The spatial profile was obtained by a high-resolution pinhole beam scan just before the lens L_1. In order to reduce the energy content of the tail of the pulse, the laser was operated with low N_2 concentrations in the gas mixture. Nevertheless, shot-to-shot changes of the energy content in the tail of the pulse resulted in an uncertainty of $\pm 20\%$ in the shot-to-shot peak power, which is the largest uncertainty present in our data. A pyroelectric detector, D_3, calibrated against the absolute energy reaching the interaction cell (IC), was used as a reference energy monitor on each shot. The beam, of variable power level, was focused into the IC containing liquid CS_2 at room temperature by the lens L_1 (shown in Fig. 1) and collected at the pinhole-detector (PHD_4) plane by the lens L_2. This setup, typical for OPL experiments, is described in greater detail in Ref. 4. The IC also contained a piezoelectric transducer, D_2, to permit the detection of the optoacoustic signal generated inside the sample by the absorption of radiation and optical breakdown of the CS_2. On the basis of previous work,[9] we expected a high sensitivity of OAD at the threshold of dielectric breakdown owing to the large increase in conversion efficiency for this case over all the other acoustic signal sources.[8]

Figure 2 shows the results of OAD up to the threshold for dielectric breakdown. The dramatic increase of the acoustic signal is observed as an abrupt steepening of the signal at the onset of breakdown. The temporal change of the transmitted pulse occurring at the breakdown threshold is also shown in Fig. 2. To show that in CS_2 the optical breakdown is SF initiated, we repeated our measurements with a different focal-length lens L_1. This varied the irradiance by a factor of 4 for a given input power. The results, presented in Fig. 3, clearly show that the onset of optical breakdown

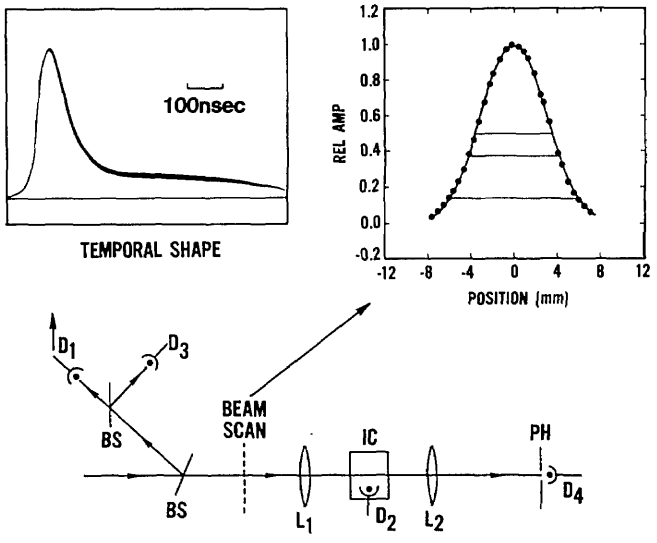

Fig. 1. Experimental setup. Lens L_1 is located so as to produce a focal spot in the middle of the interaction cell. D_1 is a photon drag detector to monitor the temporal profile of the pulse. The beam scan is performed with a 200-μm pinhole just before lens L_1. Results from a beam scan and typical temporal shape are shown.

0146-9592/85/080396-03$2.00/0

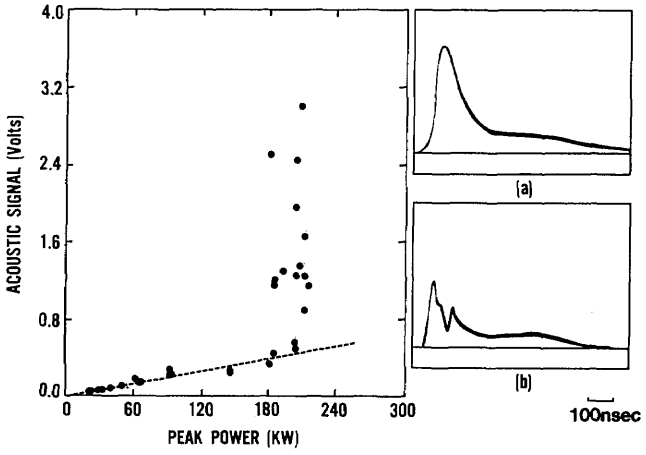

Fig. 2. Plot of measured photoacoustic signal in the interaction cell as a function of input power to the cell. Each point represents a single shot. The inset shows temporal profiles of the pulse after transmission through the cell with an input power lower (a) and greater (b) than critical power.

depends on the input power rather than on the input irradiance. The change of the index of refraction responsible for SF is irradiance dependent. Whole-beam SF results when the irradiance-dependent self-lensing overcomes diffraction. However, for a given input power both the effect of diffraction and the irradiance decrease as the focal area increases. The net result is that the power required to overcome diffraction (i.e., the critical power for SF) remains constant as the focal area changes.[10] Other nonlinear processes, such as stimulated Brillouin scattering (SBS), could, in principle, be the mechanism responsible for the large thresholdlike increase in the acoustic signal shown in Fig. 3. However, unlike SF, the onset of SBS is irradiance dependent, and the calculated irradiance threshold for the onset of SBS based on a steady-state theory[11–13] indicates a value of approximately 1.3 GW/cm^2, which could not be reached by focusing the beam with the long-focal-length lens in this experiment. Neither increased backscatter nor pump depletion characteristic of SBS was observed. These results confirm that the large acoustic signal shown in Fig. 3 is initiated by SF rather than by SBS.

The results obtained using the OPL technique were in good agreement with those obtained by OAD. The OPL results are shown in Fig. 4. In the OPL configuration at high powers the light is no longer reimaged onto the detector because of SF. In addition, the plasma created by optical breakdown of the material blocks additional light from reaching the detector. These two effects limit the energy reaching detector D_4. This limiting occurs at the same input power that produces an abrupt increase in the optoacoustic signal. Typically[4,5] in these OPL experiments what is first observed is an increase in the scatter of the data for the energy reading D_4 near the critical value for the input power, as seen in Fig. 4.

From these two measurements we extract a value for the critical power for SF of $P_c = 180 \pm 30$ kW. Marburer[10] showed with numerical computations that the critical power for SF for a focused Gaussian beam is given by $P_c = 3.77\lambda^2 c/32\pi^2 n_2$. Previous experiments have verified this relation.[4] Using our measured value of the critical power, we find that $n_2 = (2.2 \pm 0.7) \times 10^{-10}$ esu, which is to be compared with the value measured in the visible and near IR of 1.3×10^{-11} esu.[5]

Little is known about the dispersion of the nonlinear index of refraction of CS_2. On the basis of the assumption that n_2 is constant as a function of λ, one expects a λ^2 scaling of the critical power for the onset of

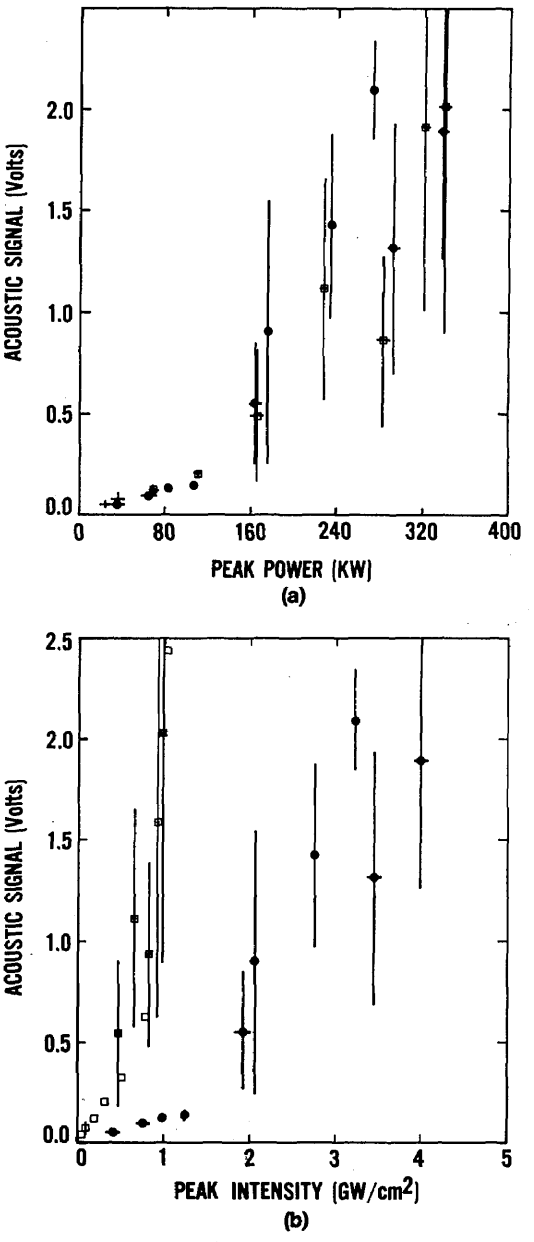

Fig. 3. (a) Photoacoustic signal versus peak power for two lenses, squares for L_1 = 12.7-cm focal-length and circles for L_1 = 6.35-cm focal-length lenses. The bars are due to averaging over many shots. The onset of the nonlinearity occurs at the same power for both lenses. Note that the value of the critical power is in agreement with Fig. 2 within the uncertainty in measurement of peak power. (b) Photoacoustic signal versus irradiance for the same two lenses.

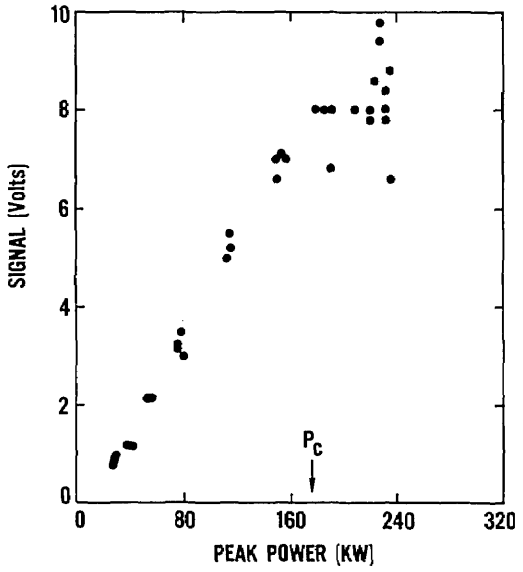

Fig. 4. Signal detected at D_4 versus peak power of the pulse in the optical-power-limiting configuration.

SF. This hypothesis has been confirmed by previous measurements in the visible and near IR. At 10.6 μm the result for n_2 reported in Ref. 7 also fits this assumption. Perhaps the reason for this agreement is that the measurement in Ref. 7 determined n_2 at the probing-beam wavelength (0.633 μm) induced in CS_2 by 10.6-μm radiation rather than n_2 at 10.6 μm. On the other hand, Ref. 6 does not supply enough information to indicate where the critical power estimate used there comes from, and, as it stands, the value of 5 kW presented in that work seems somewhat arbitrary.

Our measurements show over an order-of-magnitude increase in n_2, from 1 to 10 μm. Molecular reorientation with a response time of ~1.6 psec has long been recognized as the dominant nonlinear refractive index in the near IR and the visible. The measurement of Ref. 7 indicates that the 0.633-μm beam is still probing the same reorientational contribution.

For these pulse widths, electronic and librational contributions are small in comparison with the reorientational contribution to n_2 in the visible region and should also be small at 10.6 μm. The most likely mechanism for the observed increase in n_2 at 10 μm is the contribution of nearby vibrational resonances. Indeed, absorption from these resonances is 0.4 cm^{-1} at 10.6 μm. The presence of impurities may also explain the large observed n_2. Further studies of the dispersion of n_2 near 10.6 μm should better our understanding of the microscopic mechanisms responsible for n_2. Such experiments as well as studies of the polarization dependence are planned for the near future.

This research received support from the Defense Advanced Research Projects Agency, the Army Night Vision and Electro-Optics Laboratory, the National Science Foundation (ECS-8310625), and the North Texas State University Faculty Research Fund.

* Permanent address, Dipartimento di Elettronica, Sezione di Fisica Applicata, Universita di Pavia, Via Bassi 6, 27100 Pavia, Italy.

References

1. C. C. Wang, Phys. Rev. **152**, 149 (1966).
2. P. D. Maker and R. W. Terhune, Phys. Rev. **137**, A801 (1965).
3. K. J. Witte, M. Galanti, and R. Volk, Opt. Commun. **34**, 278 (1980.
4. M. J. Soileau, W. E. Williams, and E. W. Van Stryland, IEEE J. Quantum Electron. **QE-19**, 731 (1983).
5. W. E. Williams, M. J. Soileau, and E. W. Van Stryland, Opt. Commun. **50**, 256 (1984).
6. K. C. Jungling and O. L. Gaddy, IEEE J. Quantum Electron. **QE-7**, 97 (1971).
7. T. C. Owen, L. W. Coleman, and T. J. Burgess, Appl. Phys. Lett. **22**, 272 (1973).
8. A. C. Tam and H. Coufal, J. Phys. (Paris) **C6**, 20 (1983).
9. V. S. Teslenko, Sov. J. Quantum Electron. **7**, 981 (1977).
10. J. H. Marburger, *Progress in Quantum Electronics* (Pergamon, London, 1977), pp. 35–110.
11. H. Rabin and C. L. Tang, *Quantum Electronics* (Academic, New York, 1975), Vol. 1, Part A, Chap. 5.
12. M. Maier, Phys. Rev. **166**, 133 (1968).
13. K. Grob, Z. Phys. **201**, 59 (1967).